coatings

MDPI

Article

Recycling of Sintered NdFeB Magnet Wastes Using $Nd_{85}Al_{15}$ Alloy Diffusion

Bin Ma [1,*], Chenglong Wen [1], Jinhua Zhou [1], Yuejun Sun [1] and Aizhi Sun [2]

[1] School of Construction Machinery, ShanDong JiaoTong University, Jinan 250357, China
[2] Institute for Advanced Materials and Technology, University of Science and Technology Beijing, Beijing 100083, China
* Correspondence: 240004@sdjtu.edu.cn; Tel.: +86-17-8010-24804

Highlights

What are the main findings?

- The magnetic properties of the regenerated magnet are improved by Nd85Al15 alloy addition.
- The Nd85Al15 melt exhibited excellent wettability on the NdFeB substrate, with a contact angle below 5° above 950 °C.

What are the implications of the main findings?

- A 67.5% improvement in ultimate compressive strength was obtained in the diffused magnet.
- The addition of Nd85Al15 compensates for the deficiency of the Nd-rich phase in the recycling process.

Abstract

In this paper, the regenerated NdFeB magnets were fabricated by $Nd_{85}Al_{15}$ alloy diffusion, and the influence of alloy content and diffusion temperature on the properties and microstructure was systematically studied. The recovery mechanism of magnetic properties was discussed based on the analyses using scanning electron microscope (SEM), energy dispersive spectrometer (EDS) and electron probe microanalysis (EPMA) observation. The results indicate that the coercivity (H_{cj}) increases significantly with both alloy addition and temperature, reaching the maximum value of 1087 kA/m (80.9% enhancement) compared with the non-diffused magnet (601 kA/m). The maximum remanence (B_r) and maximum energy product (BH_{max}) of the diffused magnet are 0.99 T and 184.7 kJ/m^3, which are 8.8% and 5.9% lower than those (1.085 T and 196.3 kJ/m^3) of the non-diffused magnet. The density and compressive strength of the diffused magnet are enhanced by 8.2% (7.25 g/cm^3) and 67.47% (628 MPa), respectively. As the compensation of $Nd_{85}Al_{15}$ melt, the density, B_r and BH_{max} are improved via the liquid filling into pores. Simultaneously, the H_{cj} is enhanced through the repair of grain boundary defects and the formation of continuous Nd-rich phases.

Keywords: regenerated NdFeB magnet; coercivity; magnet wastes recycling; heat treatment

Check for updates

Academic Editor: Mikhail Avdeev

Received: 9 January 2026
Revised: 18 February 2026
Accepted: 23 February 2026
Published: 27 February 2026

Copyright: © 2026 by the authors. Licensee MDPI, Basel, Switzerland. This article is an open access article distributed under the terms and conditions of the Creative Commons Attribution (CC BY) license.

1. Introduction

Sintered NdFeB magnets exhibit the strongest energy density and are widely applied in fields of aerospace, household appliances, wind power generation and electric auto-

mobiles [1–4]. Since their invention by Sagawa in 1983 [5], the global production and accumulation of sintered NdFeB magnets have been increasing year by year, with a current total amount over 1.4 million tons [6,7]. Recently, the development of a low-carbon economy and energy-saving policies has spurred the demand for NdFeB-sintered magnets and the production of NdFeB-sintered magnets shows annual growth of more than 10% in recent years [6,8,9]. However, the fast growth simultaneously leads to a remarkable increase in storage of sintered NdFeB magnet wastes such as bulk wastes, powder wastes and sludge wastes, which are sourced from industrial wastes and end-of-life wastes; therefore, the recycling and reuse of sintered NdFeB magnet wastes has become a research hotspot in this industry [10–15].

The bulk wastes of sintered NdFeB magnets almost maintain the same structure, orientation and magnetic properties of the original magnet and display low impurities and low oxidation, which makes it possible to be recycled directly [7,16–18]. The hydrogenation technology has been applied in the recycling of bulk wastes, adopting HD (hydrogen decrepitation) or HDDR (Hydrogenation Disproportionation Desorption Recombination) processes to prepare anisotropic magneticpowders that are used to manufacture regenerated sintered magnets or bonded NdFeB magnets [7,19–21]. Li et al. [22] prepared regenerated bonded NdFeB magnets from HD-pulverized sintered magnet wastes, achieving magnetic properties of remanence (B_r) = 0.702 T, coercivity (H_{cj}) = 363 kA/m, and maximum energy product (BH_{max}) = 56.8 kJ/m^3. Zakotnik et al. [21] reported the regenerated magnets with BH_{max} = 290 kJ/m^3, B_r = 1.24 T, and H_{cj} = 830 kA/m by the HD + dehydrogenation + ball milling process. Sheridan et al. [23] combined HD with the HDDR technique to produce regenerated anisotropic NdFeB magnetic powders, the bonded magnet exhibiting B_r of 1.10 T, H_{cj} of 800 kA/m, and BH_{max} of 129 kJ/m^3. Lixandru et al. [24] demonstrated that high-quality anisotropic HDDR powders can be achieved through a two-step hydrogen treatment process (780/840 °C) with a moderate desorption rate.

In order to further improve the magnetic properties of regenerated magnets, researchers adopt hydrogenation + doping technology to reuse magnet wastes. Sun et al. [25] first produced single-crystal powders from NdFeB magnet scraps via HD and jet milling (JM) treatment, and then enhanced the coercivity through grain boundary diffusion using the low-melting-point $Ho_{69.3}Ni_{30.7}$ alloy. The best coercivity (16.35 kOe) of the regenerated magnet was obtained with the addition of 2 wt%, which is 1.24 kOe (8.2%) higher than that of the initial magnet (15.11 kOe). Liu et al. [26] prepared regenerated sintered magnets via HD and DyH_3 diffusing treatment. At 1.0 wt% DyH_3 addition, the magnet exhibited 101.7% H_{cj}, 95.4% B_r and 88.58% BH_{max} compared with the non-diffusing magnet.

In this paper, we focus on the recycling of sintered NdFeB magnet wastes by mechanical crushing and $Nd_{85}Al_{15}$ alloy diffusion, and the alloy content and diffusing temperature are systematically studied to improve the properties and microstructure of regenerated NdFeB magnets.

2. Materials and Methods

The pure Nd and pure Al with a nominal composition of $Nd_{85}Al_{15}$ in wt.% were melted in an induction furnace under an argon atmosphere and then repeated three times to prepare $Nd_{85}Al_{15}$ alloys. The polished $Nd_{85}Al_{15}$ alloy ingots were mechanically crushed under nitrogen protection and then passed through a 60-mesh sieve. The powders (20.0 g) were ball-milled in hardened stainless steel vials with 25 large balls (diameter 9.6 mm) and 50 small balls (diameter 5.8 mm) at a speed of 150 rpm for up to 2.0 h. The ball-milled powders were taken out under nitrogen protection and then passed through a 100-mesh sieve. The NdFeB wastes were mechanically crushed under nitrogen protection and passed through a 60-mesh sieve to obtain recycled magnetic powders for the

experiment. Under a nitrogen atmosphere, the recycled powders (20.0 g) with different proportions of $Nd_{85}Al_{15}$ powders (ball-milled) were mixed in vials at 60 rpm for 3.0 h. Finally, the mixed powders were placed in a BCY200 magnetic field (Baiqida Intelligent Technology, Ningbo, China) orientation press and pressed into 7.0 mm × 7.0 mm × 7.0 mm compacts under an alternating magnetic field of 1.8 T and pressure of 510 MPa. The pressed compacts were placed in a vacuum tube furnace and then heated to different temperatures for 1.0 h under 5×10^{-3} Pa, and, finally, air-cooled to room temperature to obtain the regenerated magnets.

In this study, the NIM-2000 permanent magnet measuring instrument (National Institute of Metrology, Beijing, China) was used to measure the magnetic properties of the magnets at room temperature. Before the test, the magnet was magnetized by the DZ-7 magnetizer (Beijing Zhong Ke San Huan High-tech, Beijing, China) at 5 T. The Archimedes drainage method was used to measure the density of the magnets. The calculation formula is $\rho = m_1/(m_2 - m_3)$, which requires measuring the mass of the sample in air (m_1), the mass of the vaseline-coated sample in air (m_2), and its mass in water (m_3), respectively. The morphology of the samples was observed using a FEI Quanta 450 scanning electron microscope (FEI Company, Hillsboro, OR, USA), with a working voltage of 20 kV, spot size of 5.0 nm, and vacuum level below 5×10^{-3} Pa. A DCTA21 tensiometer (Data Physics Co., Stuttgart, Germany) was employed to evaluate the wettability of the alloy on the magnet substrate. Differential scanning calorimetry (DSC) and thermogravimetry analysis (TGA) were performed on an SDT Q600 analyzer (TA Instruments, New Castle, DE, USA) with 10–20 mg samples under an argon atmosphere at a heating rate of 10 °C/min. Elemental mapping was conducted by electron probe microanalysis (EPMA, JEOL JXA-8230, Shimadzu Corporation, Kyoto, Japan).

3. Results and Discussion

3.1. Microstructural Characterization

Figure 1 presents SEM images of (a) recycled NdFeB powder obtained by mechanical crushing and (b) $Nd_{85}Al_{15}$ alloy powder after ball milling. Seen from Figure 1(a1,a2), NdFeB particles exhibit irregular, approximately spherical morphology and there are numerous defects on the particle surface, such as sharp grain edges, separation of surface Nd-rich phase (indicated by the arrows in Figure 1(a2)), grain damage and microcracks. These defects promote nucleation and growth of anti-magnetic domains to reduce magnetic properties [27,28]. Figure 1(b1,b2) reveals that the $Nd_{85}Al_{15}$ alloy particles exhibit flake-like morphology, indicating excellent plasticity and deformability. The size difference between NdFeB powders (~200 μm) and finer $Nd_{85}Al_{15}$ powders (20–30 μm) can facilitate the uniform distribution of $Nd_{85}Al_{15}$ powders on the surface of NdFeB particles.

Figure 2 shows the DSC curve of $Nd_{85}Al_{15}$ alloy, and there are two endothermic peaks at 675.37 °C and 695.17 °C, indicating the melting temperature, so the diffusion temperature in this paper should be higher than 695.17 °C. According to the Nd-Al binary phase diagram, the theoretical melting points of the $Nd_{85}Al_{15}$ and the Nd_3Al are approximately 635 °C and 675 °C, respectively. It indicates slight composition segregation during cooling and solidification. As shown in the TGA curve in the figure, the quality of $Nd_{85}Al_{15}$ alloy increases with the increase in heat treatment temperature, because the Nd-rich phase is easily oxidized [29].

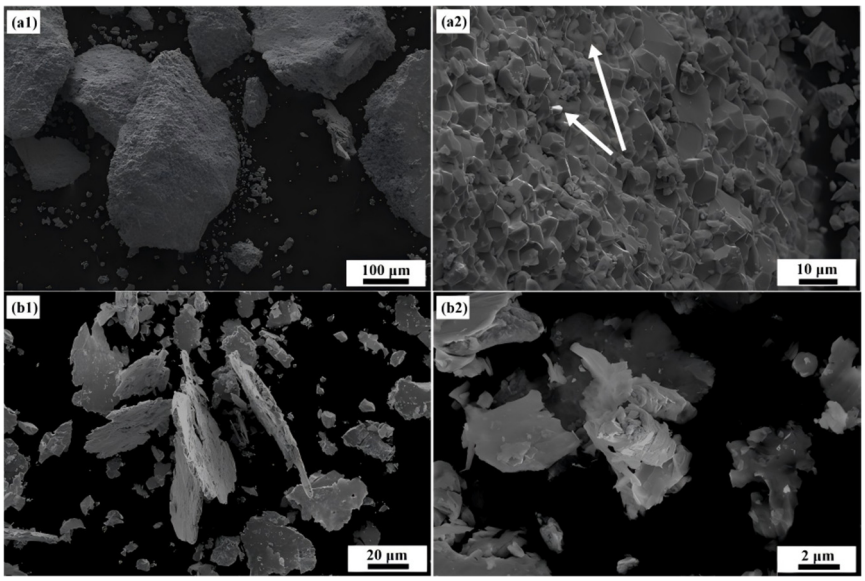


Figure 1. SEM images of the raw materials. (**a1**) SEM image of the mechanically crushed NdFeB powder; (**a2**) magnified SEM image of the mechanically crushed NdFeB powder (arrow indicates the separation of surface Nd-rich phase); (**b1**) SEM image of the ball-milled $Nd_{85}Al_{15}$ alloy powder; (**b2**) magnified SEM image of the ball-milled $Nd_{85}Al_{15}$ alloy powder.

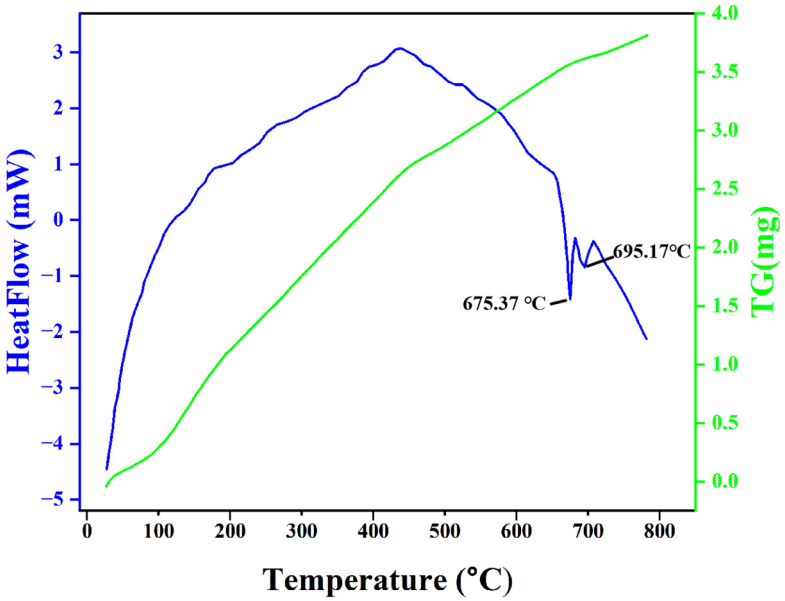


Figure 2. The DSC and TGA curves of the $Nd_{85}Al_{15}$ alloy.

3.2. Mechanical Properties

Figure 3 displays the compressive stress–strain curves of the magnets regenerated at 1040 °C: (a) with 0 wt% $Nd_{85}Al_{15}$ addition and (b) with 10.0 wt% $Nd_{85}Al_{15}$ addition. As the load pressure increases, the magnet experiences elastic-plastic deformation and, subsequently, fractures. Figure 3 demonstrates that the diffused magnet exhibits a higher compressive strength and ultimate compressive strength (628 MPa), which is 67.47% higher than the non-diffused magnet (375 MPa). The non-diffused magnet exhibits distinct plateaus at 176 MPa, 273 MPa and 298 MPa, which is characteristic of microcrack propagation. However, the disappearance of these stable regions in the diffused magnet indicates that $Nd_{85}Al_{15}$ diffusion treatment effectively repairs microstructural defects, resulting in enhanced crack resistance.

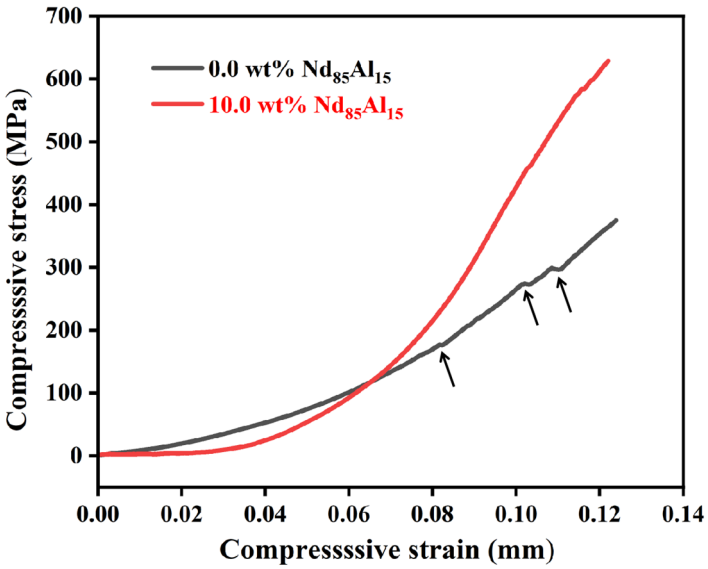


Figure 3. Compressive stress–strain curves of the magnets regenerated at 1040 °C with 0 wt% and 10 wt% $Nd_{85}A_{15}$ additions.

The wetting of the $Nd_{85}Al_{15}$ alloy solution and the NdFeB matrix determines the package of the $Nd_{85}Al_{15}$ alloy solution on NdFeB magnetic powders and the diffusion effect. Figure 4 shows the wettability of the $Nd_{85}Al_{15}$ alloy on NdFeB across the temperature range informed by the DSC curve. As shown in Figure 4, the $Nd_{85}Al_{15}$ alloy particles commenced melting and collapsing at approximately 700 °C and then the $Nd_{85}Al_{15}$ melt initiated spreading on the surface of the NdFeB magnet at 827 °C. The $Nd_{85}Al_{15}$ melt showed complete spreading on the NdFeB surface above 950 °C with a contact angle below 5°, proving the excellent wettability between the melt and the substrate. The $Nd_{85}Al_{15}$ diffusion process enhances H_{cj} by repairing defects to form a continuous grain boundary phase, while also improving the density, B_r and BH_{max}, through pore-filling.

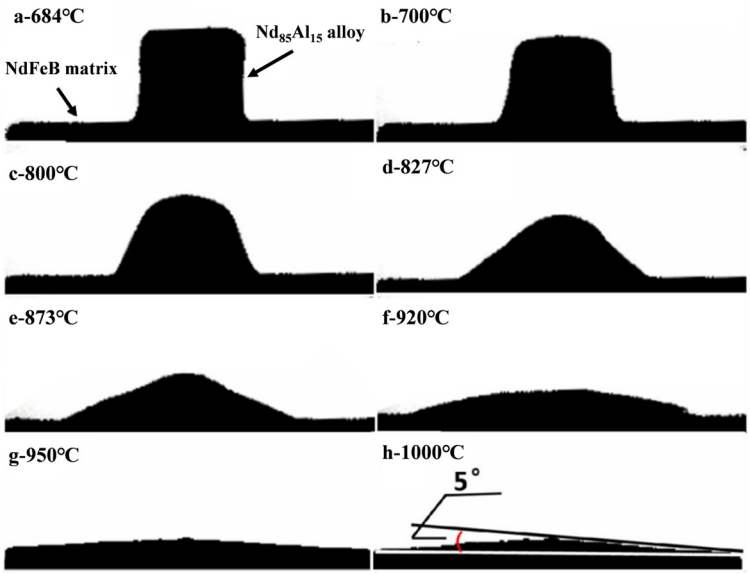


Figure 4. Wettability of the $Nd_{85}Al_{15}$ alloy on the sintered NdFeB substrate as a function of temperature: (**a**) 684 °C; (**b**) 700 °C; (**c**) 800 °C; (**d**) 827 °C; (**e**) 873 °C; (**f**) 920 °C; (**g**) 950 °C; (**h**) 1000 °C.

3.3. Magnetic Properties

Figure 5 illustrates the influence of $Nd_{85}Al_{15}$ alloy content and diffusion temperature on the magnetic properties and density of the regenerated magnet. The H_{cj} of the non-

diffused magnet (0.0 wt% $Nd_{85}Al_{15}$) increases with temperature to the maximum at 800 °C, beyond which it decreases due to high-temperature oxidation and grain coarsening [29,30]. The H_{cj} of the regenerated magnet increased continuously with both $Nd_{85}Al_{15}$ content and diffusion temperature to reach the maximum of 1087 kA/m (10.0 wt% addition at 1040 °C), which represents 80.9% enhancement over the non-diffused magnet (601 kA/m). This significant coercivity improvement is consistent with the grain boundary diffusion modification effect reported in previous studies on rare-earth-rich alloy doping for NdFeB magnet recycling [17,18,25], where the introduction of rare-earth-rich alloys effectively optimizes the grain boundary structure and enhances the magnetic isolation effect between the main phase grains. The B_r and BH_{max} increased with temperature but decreased with $Nd_{85}Al_{15}$ addition, reaching maximum values of 0.99 T and 184.7 kJ/m^3 at 5.0 wt% and 1040 °C, which are 8.8% and 5.9% below those of the non-diffused magnet (1.085 T and 196.3 kJ/m^3). The magnet density rises with increasing diffusion temperature, while it initially increases and then decreases with the addition of $Nd_{85}Al_{15}$. The maximum density of 7.25 g/cm^3 is achieved under 5.0 wt% and 1040 °C, representing an 8.2% increase compared to the non-diffused magnet (6.70 g/cm^3), which is attributed to the pore-filling effect of the molten $Nd_{85}Al_{15}$ alloy on the defective structure of recycled NdFeB powders [18,28].

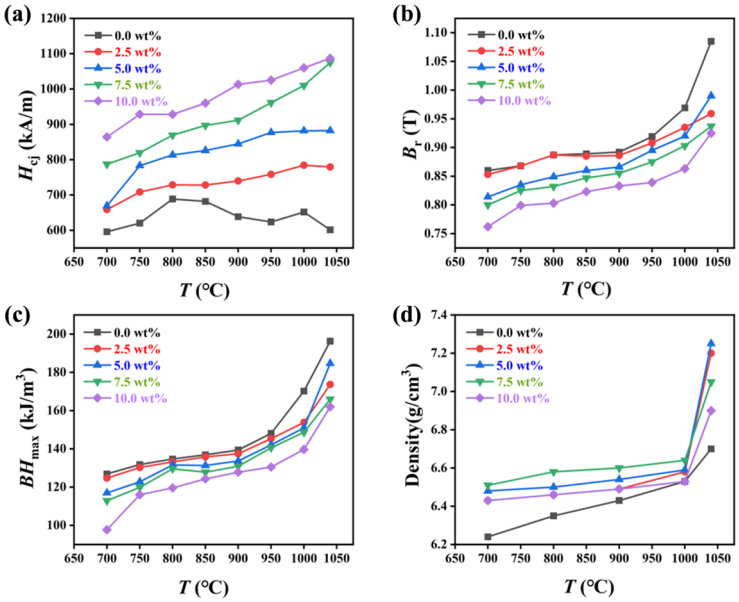


Figure 5. Effect of $Nd_{85}Al_{15}$ content and diffusion temperature on the magnetic properties and density of the regenerated magnets. (**a**) Coercivity as a function of temperature; (**b**) remanence as a function of temperature; (**c**) maximum energy product as a function of temperature; (**d**) magnet density as a function of temperature.

Figure 6 displays the microstructure of the regenerated magnet with the addition of 5 wt% $Nd_{85}Al_{15}$ after diffusion at various temperatures. As shown in the figure, smoother and denser magnets were obtained by increasing the diffusion temperature, which directly contributes to improved B_r and BH_{max} [14,31]. At 600 °C, the $Nd_{85}Al_{15}$ alloy powder remains unmelted and merely coats the magnetic particles with a resultant porous structure and low density. Although the $Nd_{85}Al_{15}$ powder melted, wetting and coating the particles at 700 °C, insufficient inward diffusion prevented significant improvement in coercivity. At 850 °C, the $Nd_{85}Al_{15}$ alloy enters the magnetic particle along the Nd-rich phase channel to repair the grain boundary and the defect area around the grain, which makes the grain surface smoother and the Nd-rich phase network more continuous and clear, resulting in an increase in coercivity. Melting of the diffusion alloy and main-phase grains at 950 °C elevates the liquid phase content, leading to enhanced grain boundary repair and

magnetic isolation for further improvement in coercivity. However, magnet shrinkage induces the accumulation of excessive Nd-rich liquid phase (indicated by the arrows in Figure 6f) at corners; the phenomenon is more obvious at 1040 °C, which is a common microstructural evolution characteristic in the high-temperature diffusion process of NdFeB magnets reported in the relevant literature [17].

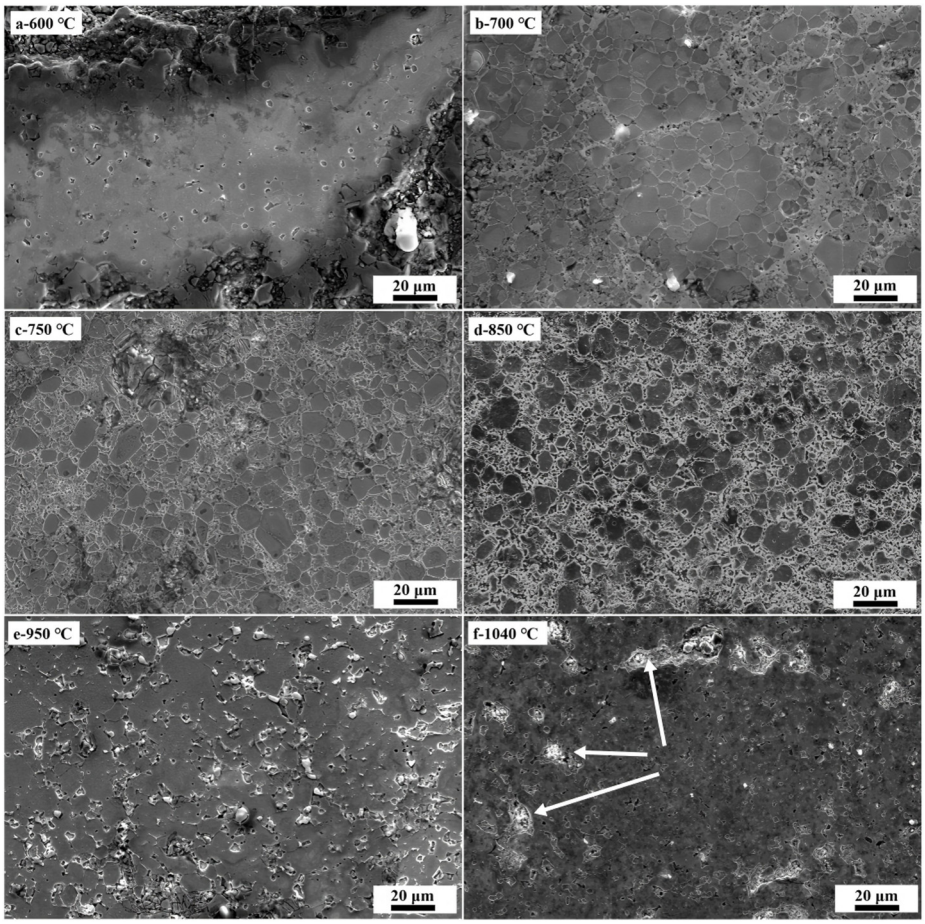


Figure 6. SEM images of the regenerated magnets with 5 wt% $Nd_{85}Al_{15}$ addition at different diffusion temperatures: (**a**) 600 °C; (**b**) 700 °C; (**c**) 750 °C; (**d**) 850 °C; (**e**) 950 °C; (**f**) 1040 °C. The arrow in (**f**) indicates the accumulation of excessive Nd-rich liquid phase.

Defects generated during the crushing process of NdFeB wastes are an important cause of decreased magnetic properties in regenerated magnets [30]. In Figure 6, the enhanced wettability of the $Nd_{85}Al_{15}$ alloy at elevated temperatures facilitates pore filling and surface defect repair, thereby improving the density, B_r and H_{cj}. With the further increase in diffusion temperature, the Nd-rich liquid phase diffuses into the magnetic powder along the grain boundaries, repairing the grain boundaries and defect regions around the grains. This enables the intergranular Nd-rich phase to distribute continuously, enhances the grain boundary magnetic isolation effect, and thus improves the coercivity of the regenerated magnets [14].

Figure 7 shows the SEM images of $Nd_{85}Al_{15}$-diffused magnets with different additive amounts and the EDS line scan analysis of the 10 wt% $Nd_{85}Al_{15}$-diffused magnet at 1040 °C. The non-diffusion magnet exhibits numerous pores and poor compactness due to the insufficient content of the Nd-rich liquid phase in Figure 7a. In Figure 7b,c, with the increase in $Nd_{85}Al_{15}$ content, the molten $Nd_{85}Al_{15}$ fills the pores and enhances the magnet density, which reaches a maximum at 5.0 wt%. However, with further addition (Figure 7d,e), excess $Nd_{85}Al_{15}$ accumulates at the triple junctions, forming large Nd-rich phases that

reduce the magnet density (indicated by the arrows in Figure 7e). Figure 7f presents a comparative analysis of the EDS line scan distributions of Al, Nd and Fe elements in the main phase grains and Nd-rich phases within the A-B region. The main phase grains in the figure exhibit the highest Fe content with relatively low Nd and Al contents, and the Nd-rich phases at the corners (a, d) show the lowest Fe and Al contents, yet the highest Nd content, forming a Fe- and Al-depleted but Nd-enriched region. In comparison with the corner Nd-rich phases, the grain boundary Nd-rich phases (b, c) have higher Fe and Al contents and a lower Nd content. This element distribution characteristic is similar to the EPMA/EDS analysis results of grain boundary diffused NdFeB magnets reported by Sepehri-Amin et al. [11] and Liu et al. [31], reflecting the selective diffusion of rare-earth-rich alloy dopants at the grain boundaries and triple junctions of NdFeB magnets.

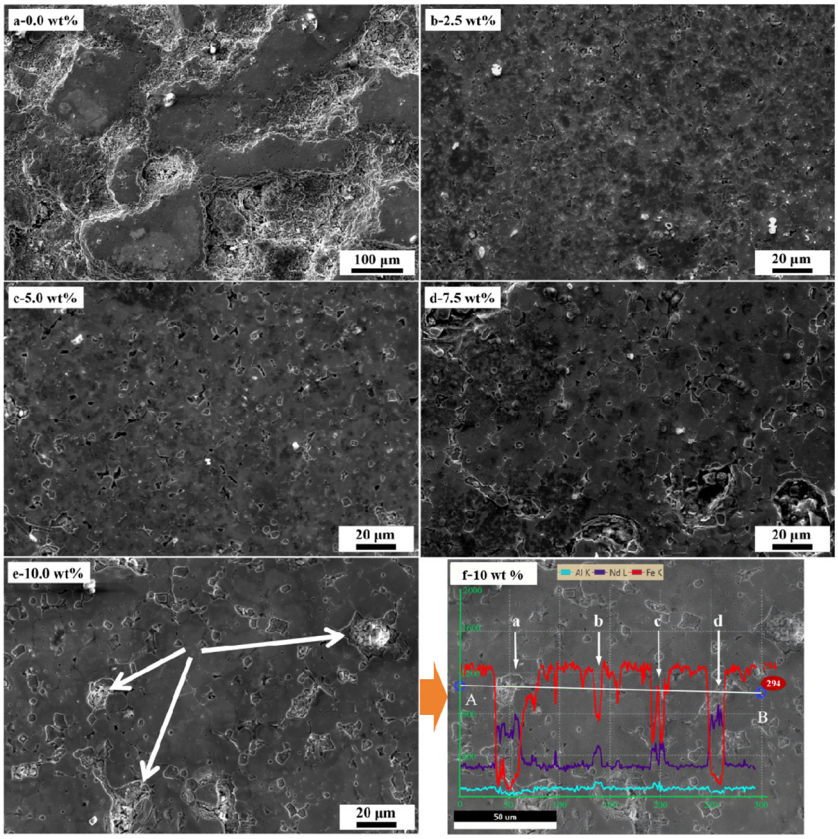


Figure 7. SEM micrographs and EDS line scan analysis of $Nd_{85}Al_{15}$-diffused magnets with different content after sintering at 1040 °C: (**a**) 0.0 wt%; (**b**) 2.5 wt%; (**c**) 5.0 wt%; (**d**) 7.5 wt%; (**e**) 10.0 wt% (arrow indicates the accumulation of excessive Nd-rich liquid phase); (**f**) 10.0 wt% $Nd_{85}Al_{15}$ addition.

The insufficient amount of Nd-rich liquid phase in the non-diffused magnets limits the improvement of magnet density and coercivity. Adding $Nd_{85}Al_{15}$ alloy supplements the Nd liquid phase, filling pores to increase density and repairing defects to enhance coercivity. However, the $Nd_{85}Al_{15}$ alloy is a non-magnetic phase and exhibits a lower density than NdFeB, leading to a decrease in density, remanence, and maximum energy product as the addition amount increases, which is a universal trade-off relationship in the grain boundary modification of NdFeB magnets with non-magnetic rare-earth-based alloys [17,26].

Figure 8 presents the EPMA element distribution of magnets diffused with 5.0 wt% $Nd_{85}Al_{15}$ alloy at 700 °C (a) and 1040 °C (b). Using the EDS line scan profiles of Al, Nd, and Fe in Figure 7f, regions A and B are identified as main-phase grains, while the arrow-highlighted areas correspond to the $Nd_{85}Al_{15}$. In the diffused magnets, Fe is predominantly enriched within the main phase grains, while Nd and Al are concentrated at the triple

junctions and grain boundaries. At 700 °C, due to the low temperature, the diffusion depth of $Nd_{85}Al_{15}$ is approximately three grain sizes, with a thin and discontinuous Nd-rich phase. At 1040 °C, the diffusion depth is increased, the Nd-rich phase becomes wider and more continuous, enhancing magnetic isolation and demagnetization coupling effects, which helps to further improve the coercivity of the magnet [17,31]. The improvement of the magnetic isolation effect by the continuous Nd-rich grain boundary phase is the key factor for the coercivity enhancement of NdFeB magnets, which has been verified by a large number of experimental and theoretical studies [11,14]. However, the diffusion of Al into the main phase grains instead of Fe will reduce B_r and BH_{max}, which is consistent with the research results of Wong et al. [27] on $Pr_{85}Al_{15}$-doped NdFeB-sintered magnets, where the slight interdiffusion of Al into the main phase leads to a minor reduction in the saturation magnetization of the main phase and, thus, a decrease in remanence.

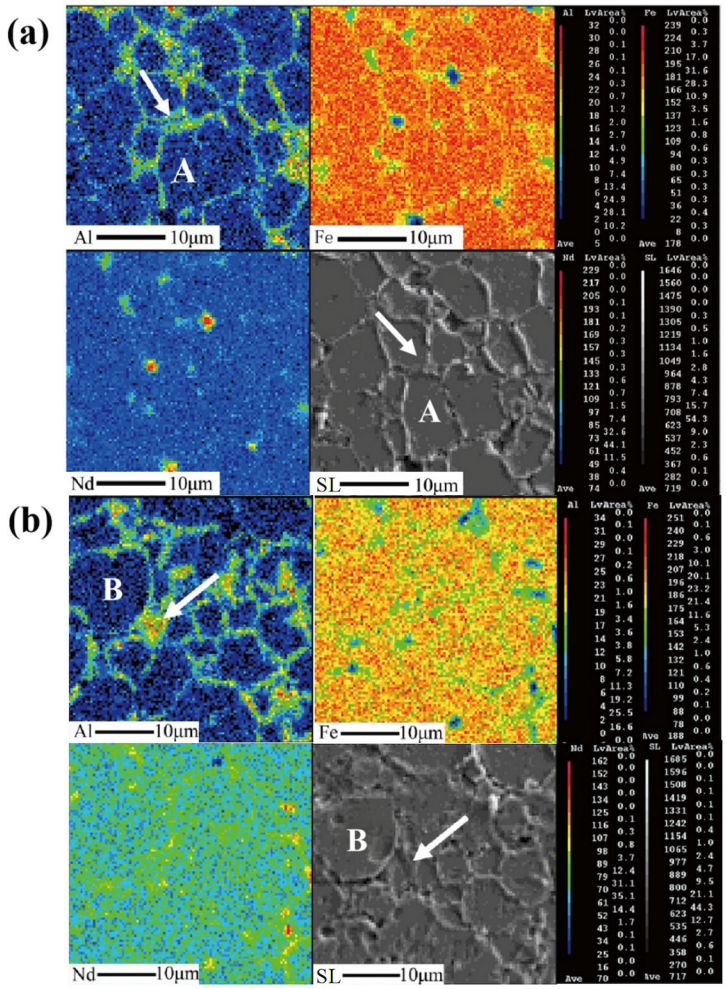


Figure 8. EPMA element distribution of magnets diffused with 5 wt% $Nd_{85}Al_{15}$ alloy at 700 °C (**a**) and 1040 °C (**b**).

4. Conclusions

This paper reports the efficient recycling of sintered NdFeB magnet wastes through $Nd_{85}Al_{15}$ alloy diffusion and investigates the effects of alloy content and diffusion temperature on the properties and microstructure.

(1) The H_{cj} of regenerated magnets increased with the $Nd_{85}Al_{15}$ content and diffusion temperature, representing 80.9% enhancement compared with the non-diffused magnet.
(2) The B_r and BH_{max} increased with diffusion temperature, while decreasing with $Nd_{85}Al_{15}$ addition, which reduced by 8.8% and 5.9% compared with the non-diffused.

(3) The compressive strength of the diffused magnet (628 MPa) displays 67.47% improvement over 375 MPa of the non-diffused magnet, resulting from the microstructure improvement by $Nd_{85}Al_{15}$ diffusion.
(4) The $Nd_{85}Al_{15}$ melt compensates for the deficiency of liquid Nd-rich phase, which improves density B_r, BH_{max} via the liquid filling into pores and simultaneously increases H_{cj} through the repair of grain boundary defects and the formation of continuous Nd-rich phases.

Author Contributions: B.M.: Methodology, Investigation, and Writing—Review and Editing. C.W.: Formal Analysis and Writing—Non-Diffused Draft. J.Z.: Funding Acquisition. Y.S.: Supervision. A.S.: Resources and Conceptualization. All authors have read and agreed to the published version of the manuscript.

Funding: This research was funded by the National Natural Science Foundation of China and the Shandong College Youth Science and Technology Program, Support grant numbers 12302059 and 2024KJH002.

Institutional Review Board Statement: Not applicable.

Informed Consent Statement: Not applicable.

Data Availability Statement: Data are contained within the article.

Conflicts of Interest: The authors declare no conflicts of interest.

References

1. Gutfleisch, O.; Willard, M.A.; Bruck, E.; Chen, C.H.; Sankar, S.G.; Liu, J.P. Magnetic materials and devices for the 21st century: Stronger, lighter, and more energy efficient. *Adv. Mater.* **2011**, *23*, 821–842. [CrossRef]
2. Zhao, M.; Liu, N.; Tang, X.; Chen, R.; Ju, J.; Yin, W.; Du, Y.; Yan, A.; Liu, X.; Pan, J.; et al. Recent progress of grain boundary diffusion process for hot-deformed Nd-Fe-B magnets. *J. Rare Earths* **2023**, *41*, 477–488. [CrossRef]
3. Zhang, D.M.; Zhu, M.G.; Zuo, J.Y.; Sun, Q.; Song, X.; Duan, Z.; Wu, X. Manipulation of the reversed domain nucleation via constructing grain size gradient distribution in Nd-Fe-B. *J. Alloys Compd.* **2025**, *1021*, 179553. [CrossRef]
4. Li, J.; Yao, Q.; Lu, Z.; Huang, W.; Chen, D.; Deng, J.; Wang, J.; Rao, G.; Zhou, H. Improvement of the coercivity and corrosion resistance of Nd-Fe-B sintered magnets by intergranular addition of $Tb_{62.5}Co_{37.5}$. *J. Magn. Magn. Mater.* **2021**, *530*, 167935. [CrossRef]
5. Sagawa, M.; Fujimura, S.; Togawa, N.; Yamamoto, H.; Matsuura, Y. New material forpermanent magnets on a base of Nd and Fe (invited). *J. Appl. Phys.* **1984**, *55*, 2083–2087. [CrossRef]
6. Hu, B.P.; Rao, X.L.; Niu, E.; Cai, D. Technology progress and industry development of rare-earth permanent magnets. *Mater. China* **2018**, *37*, 653–661, 692.
7. Yu, L.C.; Cong, L.Y.; Lu, Q.M.; Wu, Y.; Yue, M. Recent progress in recycling technology of recyclable sintered Nd-Fe-B magnets. *Chin. Rare Earths* **2023**, *44*, 72–90.
8. Liu, T.; Li, R.Y.; Zhou, L.; Shi, X.; Wei, Z. Progress of coercivity enhancement in sintered NdFeB magnets. *J. Chin. Soc. Rare Earths* **2025**, *43*, 44–56.
9. Coey, J.M.D. Perspective and prospects for rare earth permanent magnets. *Engineering* **2020**, *6*, 119–131. [CrossRef]
10. Lu, Q.; Shao, Y.; Yin, Y.; Chen, H.; Xu, H.; Liu, W.; Liu, M.; Zhong, C.; Yu, X.; Chen, J.; et al. Mass production of regenerated sintered NdFeB magnets with improved magnetic properties compared to original magnets. *Sustain. Mater. Technol.* **2023**, *36*, e615. [CrossRef]
11. Sepehri-Amin, H.; Ohkubo, T.; Zakotnik, M.; Prosperi, D.; Afiuny, P.; Tudor, C.; Hono, K. Microstructure and magnetic properties of grain boundary modified recycled Nd-Fe-B sintered magnets. *J. Alloys Compd.* **2017**, *694*, 175–184. [CrossRef]
12. Pan, M.; Liu, X.; Jin, W.; Fu, S.; Yang, E.; Liu, X.; Zhao, L.; Zhang, X.; Yan, M. Effect of Cu grain boundary modification on microstructure and corrosion resistance in recycled Nd-Fe-B sintered magnets. *J. Magn. Magn. Mater.* **2022**, *550*, 169109. [CrossRef]
13. Jin, H.Y.; Afiuny, P.; Dove, S.; Furlan, G.; Zakotnik, M.; Yih, Y.; Sutherland, J.W. Life cycle assessment of neodymium-iron-boron magnet-to-magnet recycling for electric vehicle motors. *Environ. Sci. Technol.* **2018**, *52*, 3796–3802. [CrossRef]
14. Li, X.T.; Yue, M.; Liu, W.Q.; Li, X.; Yi, X.; Huang, X.; Zhang, D.; Chen, J. Large batch recycling of waste Nd-Fe-B magnets to manufacture sintered magnets with improved magnetic properties. *J. Alloys Compd.* **2015**, *649*, 656–660. [CrossRef]

15. Yang, Y.X.; Walton, A.; Sheridan, R.; Güth, K.; Gauß, R.; Gutfleisch, O.; Buchert, M.; Steenari, B.-M.; Van Gerven, T.; Jones, P.T.; et al. REE recovery from end-of-Life NdFeB permanent magnet scrap: A critical review. *J. Sustain. Metall.* **2016**, *3*, 122–149. [CrossRef]
16. Bacchetta, G.; Luca, S.; Rado, C.; Orlandini-Keller, F.; Garandet, J. Toward the improvement of the short-loop recycling of Dy-rich Nd-Fe-B permanent magnets: Experimental and numerical approaches. *Adv. Eng. Mater.* **2024**, *26*, 2400234. [CrossRef]
17. Sun, Q.; Huang, W.; Yao, Q.; Long, Q.; Deng, J.; Wang, J.; Zhou, H. Study on the microstructure and properties of Nd-Fe-B regenerated magnet by adding $Ho_{69.3}Ni_{30.7}$ alloy at grain boundary. *J. Magn. Magn. Mater.* **2022**, *545*, 168651. [CrossRef]
18. Li, C.; Sun, A.; Tian, Z.; Zhang, X.; Ma, B. Efficient reuse of the waste sintered NdFeB magnet with Dy_2O_3 addition. *J. Magn. Magn. Mater.* **2018**, *462*, 41–45. [CrossRef]
19. Jönsson, C.; Awais, M.; Pickering, L.; Degri, M.; Zhou, W.; Bradshaw, A.; Sheridan, R.; Mann, V.; Walton, A. The extraction of NdFeB magnets from automotive scrap rotors using hydrogen. *J. Clean. Prod.* **2020**, *277*, 124058. [CrossRef]
20. Yue, M.; Yin, X.; Liu, W.; Lu, Q. Progress in recycling of Nd-Fe-B sintered magnet wastes. *Chin. Phys. B* **2019**, *28*, 77506. [CrossRef]
21. Zakotnik, M.; Harris, I.R.; Williams, A.J. Possible methods of recycling NdFeB-type sintered magnets using the HD/degassing process. *Alloys Compd.* **2008**, *450*, 525. [CrossRef]
22. Li, C.; Yue, M.; Liu, W.Q.; Zuo, T.; Yi, X.; Chen, J.; Zhou, Z.; Wu, Y. Recycling of scrap sintered Nd-Fe-B magnets as anisotropic bonded magnets via hydrogen decrepitation process. *J. Mater. Cycles Waste Manag.* **2015**, *17*, 547–552. [CrossRef]
23. Sheridan, R.S.; Sillitoe, R.; Zakotnik, M.; Harris, I.; Williams, A. Anisotropic powder from sintered Nd-Fe-B magnets by the HDDR processing route. *J. Magn. Magn. Mater.* **2012**, *324*, 63–67. [CrossRef]
24. Lixandru, A.; Poenaru, I.; Güth, K.; Gauß, R.; Gutfleisch, O. A systematic study of HDDR processing conditions for the recycling of end-of-life Nd-Fe-B magnets. *J. Alloys Compd.* **2017**, *724*, 51–61. [CrossRef]
25. Liu, L.; Sepehri-Amin, H.; Ohkubo, T.; Yano, M.; Kato, A.; Sakuma, N.; Shoji, T.; Hono, K. Coercivity enhancement of hot-deformed Nd-Fe-B magnets by the eutectic grain boundary diffusion process using $Nd_{62}Dy_{20}Al_{18}$ alloy. *Scr. Mater.* **2017**, *129*, 44–47. [CrossRef]
26. Liu, W.; Li, C.; Zakotnik, M.; Yue, M.; Zhang, D.; Huang, X. Recycling of waste Nd-Fe-B sintered magnets by doping with dysprosium hydride nanoparticles. *J. Rare Earths* **2015**, *33*, 846–849. [CrossRef]
27. Wong, Y.J.; Lin, B.S.; Chang, H.W.; Chiu, C.; Mo, C. Enhancement of coercivity and thermal stability of $Pr_{85}Al_{15}$ doped NdFeB sintered magnets followed with grain boundary diffusion. *J. Magn. Magn. Mater.* **2023**, *571*, 170562. [CrossRef]
28. Chao, L.; Wei, Q.L.; Ming, Y.; Liu, Y.Q.; Zhang, D.T.; Zuo, T.Y. Waste Nd-Fe-B Sintered Magnet Recycling by Doping with Rare Earth Rich Alloys. *IEEE Trans. Magn.* **2014**, *50*, 1–3. [CrossRef]
29. Edgley, D.S.; Le Breton, J.M.; Steyaert, S.; Ahmed, F.; Harris, I.; Teillet, J. Characterisation of high temperature oxidation of NdFeB magnets. *J. Magn. Magn. Mater.* **1997**, *173*, 29–42. [CrossRef]
30. Kwon, H.W.; Jeong, I.C.; Kim, A.S.; Kim, D.; Namkung, S.; Jang, T.; Lee, D. Restoration of coercivity in crushed Nd-Fe-B magnetic powder. *J. Magn. Magn. Mater.* **2006**, *304*, e219–e221. [CrossRef]
31. Liu, L.; Sepehri-Amin, H.; Ohkubo, T.; Yano, M.; Kato, A.; Shoji, T.; Hono, K. Coercivity enhancement of hot-deformed Nd-Fe-B magnets by the eutectic grain boundary diffusion process. *J. Alloys Compd.* **2016**, *666*, 432–439. [CrossRef]

Disclaimer/Publisher's Note: The statements, opinions and data contained in all publications are solely those of the individual author(s) and contributor(s) and not of MDPI and/or the editor(s). MDPI and/or the editor(s) disclaim responsibility for any injury to people or property resulting from any ideas, methods, instructions or products referred to in the content.